Levels and gamma energies of ^{28}Al studied by thermal neutron capture

H. H. Schmidt, P. Hungerford, H. Daniel, and T. von Egidy
Physik-Department, Technische Universität München, Munich, Germany

S. A. Kerr, R. Brissot, G. Barreau, H. G. Börner, and C. Hofmeyr*
Institut Laue-Langevin, Grenoble, France

K. P. Lieb
2. Physikalisches Institut, Universität Göttingen, Göttingen, Germany
(Received 4 February 1982)

The ^{27}Al$(n,\gamma)^{28}$Al reaction has been studied using curved crystal spectrometers, a pair spectrometer, and a Ge(Li) detector. Applying a self-consistent energy calibration, a set of 199 calibration energies relative to the 411 keV Au standard was obtained. An extensive level scheme up to 8 MeV has been established. The neutron binding energy was determined to be 7725.18 ± 0.09 keV. The energy of the ^{28}Si transition following the β decay of ^{28}Al was found to be 1778.987 ± 0.015 keV.

[NUCLEAR REACTIONS ^{27}Al(n,γ); E_n = thermal; measured E_γ, I_γ; deduced levels, J,π. Crystal spectrometer, Ge(Li).]

I. INTRODUCTION

The odd-odd nucleus ^{28}Al lies in the transition region of prolate and oblate deformations in the *sd* shell. It has been found that many of the low lying states of nuclei in this interesting region can be described by the shell model.[1,2] However, for ^{28}Al ambiguities remain in the level scheme[3] and there is a lack of precise low energy gamma ray data. Previous (n,γ) work[4–8] has been either limited in its precision or has not been primarily concerned with nuclear structure effects. In addition to the nuclear structure aspects, precise values for the energies and the intensities of gamma rays emitted by ^{28}Al are of interest since they are often present as background lines in neutron capture measurements. Thus accurate values would allow for their identification, as well as provide a possible energy calibration.

The ^{27}Al$(n,\gamma)^{28}$Al reaction was studied at the high flux reactor of the Institute Laue-Langevin (ILL), Grenoble, using the GAMS crystal spectrometers[9] for the low-energy part of the gamma ray spectrum and a pair spectrometer[10] for the higher energies. Furthermore, the low energy transitions were measured with a Ge(Li) detector at an external neutron guide.[11] The measurements were performed with pure aluminium and with mixed targets containing aluminium and chlorine in order to calibrate the ^{28}Al spectra with the ^{36}Cl energies. These energies have recently been measured with high precision[12] relative to the 411 keV ^{198}Au decay standard.[13]

II. EXPERIMENTAL DETAILS

A. The Ge(Li) measurements

The Ge(Li) measurements were performed at the end position of the thermal neutron guide H22 at the ILL. The neutron flux at this position is about 4×10^7 cm^{-2}s^{-1}. The target was a sheet of 99.999% pure aluminium with the dimensions $2\times1\times0.1$ cm^3. The gamma rays emitted were detected by a coaxial Ge(Li) detector of 20% efficiency and 2.5 keV FWHM at 1.3 MeV. The spectra were recorded in the energy range between 80 and 2200 keV. In addition, background measurements were undertaken using a dummy target. The relative detector efficiency was determined from the ^{152}Eu decay.[14]

B. The GAMS measurements

The GAMS measurements were carried out by the curved crystal spectrometers GAMS.[9] Two targets were used, one consisting of 99.999% pure aluminium metal and one consisting of a homogeneous mixture of lead fluoride, potassium chloride, and aluminium metal contained in a pure aluminium target holder. The targets were situated in a thermal neutron flux of 5.5×10^{14} cm^{-2}s^{-1}. The spectra were recorded in the first five orders of reflection. The FWHM was 240 eV for the 400.5 keV line in the second order. For the measurements with the pure Al target the energy values of the Al lines obtained by a preliminary energy calibration of the Ge(Li) spectrum were taken for the determination of the angular ranges to be scanned with GAMS. The GAMS intensities were calibrated using the intensities obtained by the Ge(Li) measurement and both values were used to obtain the final intensities.

C. The pair spectrometer measurements

The gamma spectra were also measured with the pair spectrometer facility at the ILL.[10] The target position was the same as for the GAMS measurements. Again two targets were used, one pure aluminium target and one mixed target. The Al target consisted of 1.83 g 99.999% pure Al metal. The mixed target was the same as for the GAMS measurements. The spectra were recorded between 1.4 and 8 MeV and an energy resolution of 5.5 keV at 7.7 MeV was achieved. Figure 1 shows a part of the ^{28}Al spectrum. The intensities were obtained using an analytical efficiency function.[15] The parameters of this function were previously determined relative to a set of nitrogen lines.[16] Assuming that the total gamma intensity is included in the level scheme, the intensities I_i were normalized using

$$\frac{\sum_i E_i I_i}{E_B} = 100\% ,$$

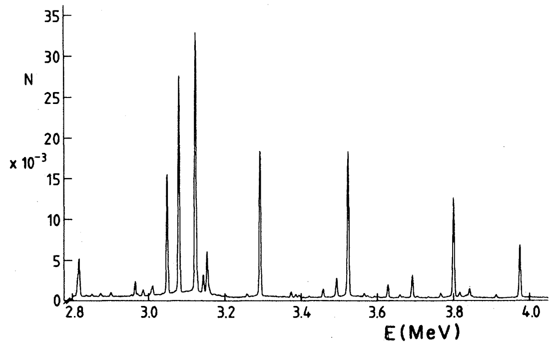

FIG. 1. Part of the pair spectrum of ^{28}Al.

where the E_i are the gamma ray energies and E_B is the neutron binding energy.

III. ENERGY CALIBRATION AND SYSTEMATIC ERROR

A. Energies below 2.2 MeV

For the determination of the gamma energies from 0 to 2.2 MeV the GAMS and Ge(Li) measurements were used. The energy calibration was undertaken with the GAMS measurement because it is possible to obtain absolute energies apart from a common constant factor using the different orders of reflection of the measured lines.[9] To determine the common factor the spectrum of the mixed target was used to calibrate the 1779 keV ^{28}Al decay line relative to the 517.077 ± 0.001 keV ^{36}Cl line, which in turn had been previously determined relative to the 411 keV Au line.[12] By means of these absolute energy values the energies obtained by the Ge(Li) measurement were calibrated. Both values were then used to obtain the final energies.

B. Energies above 2.2 MeV

All transitions with energies above 2.2 MeV were only measured with the pair spectrometer. No absolute calibration method as in the case of the GAMS measurements is available and the nonlinearity of the system exceeds by far the statistical errors. However, as the level scheme connects the energies above 2.2 MeV strongly to those below 2.2 MeV, which are known on an absolute scale (Sec. III A), an iterative procedure can be used, always renormalizing the energies above 2.2 MeV to the corresponding level energy differences. This was performed in the following manner: As a starting point, the energies above 2.2 MeV of the ^{28}Al spectrum were calibrated to the ^{36}Cl spectrum.[12] Then with this set of line energies above 2.2 MeV and the line energies below 2.2 MeV (Sec. III A), the level energies were determined by a least squares fit. Then the lines above 2.2 MeV were recalibrated using the energy differences of the corresponding levels. This calibration was done for four separate energy regions always using a quadratic polynomial, because it was not possible to fit the nonlinearity with a simple analytical function over the whole energy range from 2 to 8 MeV. The boundaries of these regions were chosen in such a way that there is a smooth overlap between the adjacent ones. The new set of line energies consisting of the recalibrated ones above 2.2 MeV and the initial ones below 2.2 MeV was then used again to determine the level energies. The whole procedure was repeated three times. The last iteration only changed the energies by less than 15 eV. In this way, a self-consistent set of energies was obtained, energies which are nearly independent of the ^{36}Cl calibration of the pair spectrometer and are relative to the 411 keV Au standard.

Using the final energy set, a reduced χ^2 value of 2.4 was obtained for the fit of the level energies to the transition energies. As the number of the degrees of freedom is about 150 this value for the χ^2 definitely shows that there are nonstatistical errors included in the system. These errors could be due to wrongly placed lines in the level scheme, unresolved doublets, incorrectly assumed background, or to remaining nonlinearities in the calibration of the pair spectrometer. To obtain an estimation of the systematic error which accounts for these nonlinearities, a special procedure was used, which relies on the strong interconnections between the transition energies via the level scheme. The idea is, to test the effect of artificially introduced systematic deviations of the transition energies on the χ^2 obtained by the fit of the level energies to the transition energies. In order to do this, a kink was introduced into the calibration curve, so that the transition energies above a certain energy E_0 had a linearly increasing deviation $[E'=E+\alpha(E-E_0)$ for $E>E_0$ and $E'=E$ for $E\leq E_0]$. For different values of the parameters E_0 and α, the variation of the χ^2 was determined. The most pronounced change was obtained for $E_0=4000$ keV. Figure 2 shows the χ^2 as a function of α for $E_0=4000$ keV. The almost symmetric shape of the curve indicates that the nonlinearity introduced into the system by replacing the energies E by E' is independent of the nonlinearities already present. Therefore, as the χ^2 for the undisturbed system exceeds its expectation value by 1.4, an artificially introduced nonlinearity of $\alpha=\pm3.3\times10^{-5}$, which causes an increase of the χ^2 by another 1.4, is an estimate for the nonlinearities already present. For $\alpha=\pm3.3\times10^{-5}$ the fitted value of the binding energy changed by about 80 eV. Considering the fact that the lower energies are more precisely determined by the absolute GAMS energies and taking into account that only a part of the increase of the χ^2 is due to remaining nonlinearities, a systematic error of 8 ppm is estimated for the energies above 2.2 MeV. An additional 8 ppm uncertainty due to the statistical error of the 1779 keV line has been considered to obtain the final errors on the absolute energy values. This error has to be taken into account for all energies, so that the systematic error amounts to 8 ppm for the energies below 2.2 MeV and to 11 ppm for the energies above 2.2 MeV. In this way, a total error of 90 eV is obtained for the neutron binding energy.

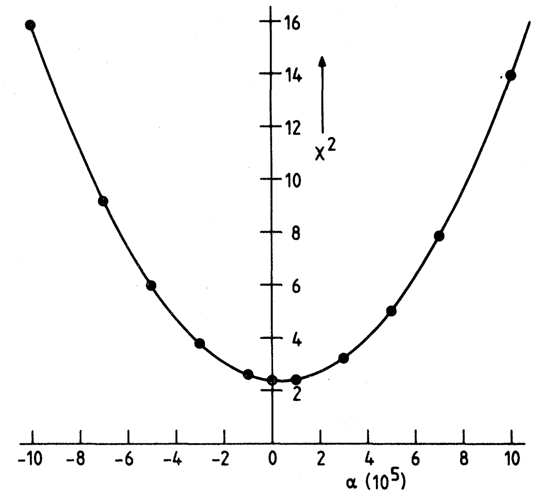

FIG. 2. Variation of the χ^2 for the level fit as a function of α (see text).

IV. RESULTS

A. Measured and recommended energies

The neutron binding energy and the energy of the ^{28}Al decay line have been determined to be 7725.18 ± 09 and 1778.987 ± 0.015 keV, respectively. In total, 278 ^{28}Al transitions have been observed. The sensitivity of the measurements is about 0.2 gammas per 100 neutron captures in the region up to 2.2 MeV and about 0.002 gammas per 100 neutron captures in the region above 2.2 MeV. A total of 199 lines have been placed in the level scheme. Table I shows the line energies and intensities. For lines placed in the level scheme the corresponding difference in level energy is also given. These latter energies are recommended as calibration energies. The energy errors given in Table I are purely statistical. As pointed out in Sec. III B a systematic error of 8 ppm for the energies below 2.2 MeV and 11 ppm for the energies above 2.2 MeV should be added. The intensity errors include a systematic error of 10% for the lines below 2.2 MeV and of 5% for the lines above 2.2 MeV.

TABLE I. Measured gamma energies and intensities and recommended calibration energies. Only statistical energy errors are given. In order to obtain total energy errors 8 or 11 ppm has to be added in quadrature below or above 2.2 MeV, respectively.

Gamma energy[a] (keV)	Calibration energy[b] (keV)	Intensity/100n	Gamma energy[a] (keV)	Calibration energy[b] (keV)	Intensity/100n
30.6382(7)	30.6382(7)	c	2313.3(3)[d]	2312.56(5)	0.035(6)
400.58(3)	400.573(22)	0.63(7)	2347.38(10)	2347.27(4)	0.16(1)
455.68(18)	455.70(5)	0.29(7)	2380.34(5)	n	0.21(1)
548.70(13)	548.69(4)	0.23(3)	2384.3(3)	n	0.034(6)
647.9(12)[d]	647.94(5)	0.07(4)	2419.36(8)	2419.22(3)	0.14(1)
831.45(4)	831.464(20)	1.3(2)	2451.48(4)	2451.554(18)	0.39(2)
865.88(15)	865.84(5)	0.54(7)	2455.8(3)[d]	2455.42(3)	0.036(7)
941.79(6)	941.72(3)	1.3(1)	2486.09(7)	2486.058(19)	0.18(1)
945.1(5)	945.34(7)	0.24(7)	2502.85(7)	2502.71(4)	0.16(1)
968.71(15)	968.49(6)	0.42(6)	2534.62(12)	2534.92(16)	0.084(8)
983.018(16)	982.968(23)	4.4(5)	2548.08(8)	2548.09(5)	0.15(1)
1013.676(21)	1013.605(25)	2.7(3)	2552.07(12)	2552.060(10)	0.094(8)
1073.87(11)	1073.99(5)	0.57(7)	2563.51(23)	2563.32(3)	0.10(1)
1101.8(4)	1102.08(4)	0.7(2)	2567.8(3)	n	0.70(1)
1125.54(21)	1125.266(14)	0.38(7)	2577.725(21)	2577.696(13)	2.2(1)
1173.4(3)	1173.440(9)	0.39(9)	2582.2(5)	2581.90(19)	0.05(1)
1193.64(10)	1193.500(23)	0.6(1)	2590.244(14)	2590.212(17)	4.2(2)
1283.54(7)	1283.70(3)	1.1(1)	2625.903(16)	2625.866(23)	1.37(7)
1304.8(3)	1305.30(12)	0.19(5)	2656.34(7)	n	0.16(1)
1342.30(11)	1342.280(18)	1.0(1)	2691.0(3)	2690.65(5)	0.029(6)
1364.99(20)	1364.62(14)	0.38(6)	2709.665(20)	2709.62(4)	0.69(4)
1373.3(5)[d]	1372.917(18)	0.15(8)	2717.4(4)[d]	n	0.021(5)
1408.30(6)	1408.346(9)	3.1(3)	2724.6(5)	2725.206(13)	0.021(6)
1526.17(11)	1526.258(12)	1.8(2)	2728.27(5)	n	0.27(1)
1589.72(8)	1589.64(5)	1.6(2)	2733.64(3)	n	0.38(2)
1592.29(12)	1592.235(18)	0.36(5)	2743.74(19)	2743.51(3)	0.045(6)
1622.87(6)	1622.871(18)	4.6(5)	2821.461(16)	2821.454(7)	3.9(2)
1642.35(10)	1642.41(3)	0.30(5)	2862.24(22)	2862.000(11)	0.038(6)
1673.43(11)	1673.411(22)	0.23(3)	2876.29(8)	2876.44(11)	0.116(8)
1705.38(8)	1705.52(4)	0.39(5)	2881.2(3)	2880.73(7)	0.027(5)
1720.0(3)[d]	m	0.08(5)	2887.22(4)	2887.208(25)	0.23(1)
1864.59(22)	1864.33(3)	0.46(7)	2893.87(17)	n	0.049(6)
1927.87(16)	1927.56(3)	1.2(2)	2902.7(7)[d]	2903.24(3)	0.011(5)
1963.68(20)[d]	n	0.05(1)	2921.84(3)	2921.795(17)	0.28(1)
1968.35(12)	1968.452(19)	0.10(1)	2954.88(19)	2954.38(18)	0.23(3)
1975.2(5)[d]	m	0.025(8)	2960.114(11)	2960.099(10)	9.6(5)
1983.99(20)	1983.990(13)	1.1(1)	2974.0(3)	2973.42(7)	0.024(3)
2047.70(23)	2047.77(4)	0.07(1)	2987.69(17)	2987.41(12)	0.32(4)
2108.24(4)	2108.192(11)	2.8(1)	3016.7(7)	3017.75(3)	0.06(2)
2128.81(7)	2128.70(3)	0.34(2)	3020.3(7)	3020.235(15)	0.07(2)
2138.828(18)	2138.828(9)	2.2(1)	3023.8(8)	3024.89(13)	0.05(2)
2170.70(3)	2170.74(3)	0.45(3)	3033.893(13)	3033.904(6)	8.8(4)
2247.21(23)[d]	2247.39(3)	0.040(6)	3053.6(4)[d]	n	0.021(5)
2255.42(5)	2255.36(5)	0.55(4)	3068.16(10)	3068.00(3)	0.081(6)
2271.650(23)	2271.667(16)	2.1(1)	3075.65(9)	n	0.083(6)
2276.7(11)[d]	m	0.04(3)	3128.51(4)	3128.48(3)	0.24(1)
2279.1(7)	n	0.08(3)	3142.22(6)	n	0.16(1)
2282.773(14)	2282.804(15)	4.7(2)	3191.20(12)	n	0.048(3)
2299.94(10)	n	0.12(1)	3208.27(7)	n	0.092(6)

TABLE I. (Continued.)

Gamma energy[a] (keV)	Calibration energy[b] (keV)	Intensity/100n	Gamma energy[a] (keV)	Calibration energy[b] (keV)	Intensity/100n
3222.83(12)	3222.73(4)	0.049(3)	4059.78(19)	4059.647(14)	0.030(3)
3230.68(20)	3230.59(8)	0.027(3)	4068.99(4)	4069.007(19)	0.157(8)
3254.9(3)	3254.736(23)	0.022(3)	4085.1(5)	4085.17(8)	0.008(2)
3263.18(16)	3263.06(8)	0.10(1)	4101.7(5)	4100.26(15)	0.016(5)
3265.49(4)	3265.544(17)	0.42(3)	4119.9(4)	*m*	0.040(8)
3303.150(13)	3303.153(9)	1.14(6)	4125.09(22)	*n*	0.088(9)
3316.5(3)	3316.341(12)	0.025(3)	4133.408(8)	4133.406(6)	6.9(3)
3346.978(18)	3346.975(12)	0.50(3)	4162.4(5)	*m*	0.019(5)
3375.08(24)	*n*	0.026(3)	4169.38(6)	4169.347(19)	0.122(7)
3392.00(10)	3391.74(5)	0.57(3)	4175.06(23)	*n*	0.030(3)
3409.2(3)	3409.26(5)	0.023(3)	4185.23(10)	*n*	0.064(5)
3448.03(23)	3448.06(8)	0.032(5)	4213.49(11)	4213.43(8)	0.056(3)
3465.067(10)	3465.063(7)	7.0(4)	4218.04(22)	4218.04(7)	0.027(3)
3472.3(3)	*n*	0.06(1)	4237.43(10)	*m*	0.060(5)
3480.77(16)	3480.54(12)	0.12(1)	4259.539(8)	4259.539(6)	6.8(3)
3560.547(19)	3560.567(7)	0.93(5)	4270.1(3)	4270.14(5)	0.054(7)
3569.9(3)	*n*	0.036(6)	4280.37(10)	4280.58(15)	0.17(1)
3591.211(11)	3591.201(6)	4.7(2)	4330.75(12)	*n*	0.052(3)
3598.66(12)	3598.46(10)	0.15(1)	4377.625(16)	4377.624(12)	0.43(2)
3623.74(7)	3623.88(7)	0.086(6)	4384.1(4)[d]	*n*	0.010(2)
3634.8(6)[d]	3635.24(8)	0.010(3)	4396.40(6)	4396.32(4)	0.058(3)
3639.88(9)	3639.88(4)	0.073(5)	4424.24(3)	4424.221(20)	0.36(2)
3659.08(9)	3659.06(3)	0.064(5)	4428.410(13)	4428.418(12)	0.81(4)
3671.22(8)	*n*	0.070(5)	4447.27(19)	*n*	0.019(2)
3678.15(5)	3678.32(3)	0.31(2)	4461.60(10)	4461.54(8)	0.042(3)
3702.22(7)	*n*	0.078(5)	4484.53(6)	4484.52(5)	0.071(5)
3708.976(16)	3708.953(15)	0.45(2)	4511.86(5)	4511.86(4)	0.084(5)
3721.52(22)	3721.60(3)	0.030(3)	4565.67(15)	4565.47(3)	0.027(2)
3725.1(3)	*n*	0.024(3)	4575.557(21)	4575.555(17)	0.30(2)
3750.83(18)	*m*	0.035(3)	4582.21(11)	*n*	0.041(3)
3754.70(15)	3754.62(4)	0.043(3)	4596.14(4)	4596.11(3)	0.124(7)
3768.6(4)	3768.82(9)	0.013(2)	4613.2(4)	4612.98(6)	0.016(2)
3789.331(14)	3789.322(11)	0.87(4)	4617.77(12)	*n*	0.082(6)
3803.7(5)	3803.74(5)	0.011(3)	4621.47(5)	4621.53(3)	0.19(1)
3820.9(4)	3821.67(8)	0.033(8)	4660.039(8)	4660.046(5)	2.6(1)
3823.90(3)	3823.908(24)	0.56(3)	4690.677(7)	4690.678(5)	4.6(2)
3849.108(10)	3849.114(7)	3.1(2)	4733.847(12)	4733.846(7)	5.5(3)
3859.47(24)	3859.1(3)	0.046(6)	4737.40(9)	4737.17(18)	0.45(2)
3865.7(4)[d]	*n*	0.027(6)	4754.24(4)	4754.35(6)	0.38(2)
3875.480(11)	3875.495(10)	2.7(1)	4764.45(3)	4764.479(8)	0.91(5)
3881.8(4)[d]	*n*	0.027(6)	4769.61(15)	*n*	0.113(9)
3889.73(6)	3889.659(12)	0.23(1)	4783.0(5)	4783.485(18)	0.011(3)
3900.65(7)	3900.701(24)	0.23(1)	4812.54(17)	*n*	0.031(2)
3904.76(8)	3904.653(14)	0.20(1)	4868.80(9)	*n*	0.058(3)
3926.86(24)	3926.816(19)	0.023(3)	4903.115(6)	4903.113(6)	3.1(2)
3935.276(23)	3935.287(11)	0.33(2)	4965.8(4)[d]	*n*	0.009(1)
3949.8(4)	*n*	0.014(2)	4984.30(4)	4984.308(17)	0.113(6)
4001.70(5)	4001.49(8)	0.135(8)	4996.64(7)	*n*	0.064(3)
4015.664(14)	4015.655(10)	0.73(4)	5005.45(9)	5005.504(24)	0.048(3)
4023.21(5)	*n*	0.138(8)	5016.5(12)[d]	5014.940(21)	0.003(1)
4045.00(23)	4044.716(22)	0.023(2)	5031.51(17)	*n*	0.017(1)
4054.04(5)	4054.09(4)	0.143(8)	5068.58(3)	5068.60(3)	0.173(9)

TABLE I. (*Continued.*)

Gamma energy[a] (keV)	Calibration energy[b] (keV)	Intensity/100*n*	Gamma energy[a] (keV)	Calibration energy[b] (keV)	Intensity/100*n*
5103.718(15)	5103.702(7)	0.39(2)	5969.54(15)	*n*	0.023(2)
5130.40(15)	5130.06(11)	0.107(9)	5988.32(15)	5988.284(23)	0.023(2)
5134.342(9)	5134.334(7)	3.0(1)	6018.88(3)	6018.92(3)	0.187(9)
5141.8(4)	5142.6(4)	0.015(2)	6101.40(5)	6101.54(5)	2.6(1)
5176.44(6)	5176.45(5)	0.070(3)	6109.6(7)	*n*	0.010(2)
5184.99(13)	5184.74(3)	0.030(2)	6121.3(5)	*n*	0.011(2)
5203.54(21)	*n*	0.017(1)	6161.8(3)	6162.13(4)	0.013(2)
5209.30(24)	*n*	0.022(2)	6198.138(12)	6198.141(11)	0.67(3)
5213.4(5)	*n*	0.009(2)	6210.8(3)	*n*	0.013(1)
5228.4(4)	*n*	0.008(1)	6255.05(23)	6255.10(5)	0.014(1)
5238.481(20)	5238.478(19)	0.26(1)	6289.6(8)^d	*n*	0.003(1)
5269.91(6)	*n*	0.057(3)	6316.017(10)	6316.031(12)	2.0(1)
5277.56(16)	5277.68(5)	0.021(1)	6329.5(8)	*n*	0.008(2)
5302.650(14)	5302.632(12)	0.47(2)	6351.36(4)	6351.45(4)	0.109(6)
5315.14(12)	*n*	0.031(2)	6390.2(5)^d	*n*	0.008(1)
5344.24(17)	5343.87(6)	0.017(1)	6420.0(5)^d	6419.06(12)	0.006(1)
5377.27(4)	5377.25(4)	0.080(5)	6440.648(11)	6440.651(11)	0.66(3)
5411.069(8)	5411.077(7)	2.0(1)	6449.5(5)^d	*n*	0.007(1)
5427.19(7)	5427.257(13)	0.087(5)	6459.69(22)	*n*	0.016(1)
5441.9(3)	5441.70(7)	0.015(2)	6591.61(4)	6591.61(4)	0.164(9)
5446.88(15)	5446.90(7)	0.035(2)	6619.59(14)	6619.69(4)	0.24(2)
5452.77(3)	5452.84(4)	0.168(9)	6621.79(18)	6622.24(9)	0.19(2)
5459.39(18)	*n*	0.021(2)	6628.4(5)	*n*	0.011(2)
5522.96(6)	5523.13(7)	0.064(3)	6710.702(15)	6710.692(7)	0.90(5)
5564.6(5)^d	*n*	0.007(1)	6725.15(8)	6725.16(5)	0.086(5)
5585.54(5)	5585.667(23)	1.10(5)	6752.32(12)	6751.93(8)	0.058(3)
5594.7(4)	*n*	0.009(1)	6800.7(3)	*n*	0.022(2)
5709.852(13)	5709.852(13)	0.56(3)	6823.03(11)	*n*	0.055(3)
5719.14(16)	*n*	0.022(2)	6862.22(4)	6862.16(3)	0.173(9)
5729.6(4)	*n*	0.008(1)	6894.27(17)	*n*	0.031(2)
5748.2(14)^d	*n*	0.002(2)	6936.97(5)	*n*	0.124(7)
5760.57(24)	*n*	0.023(2)	7135.24(12)	*n*	0.054(3)
5766.250(22)	5766.272(17)	0.38(2)	7175.53(5)	7175.50(4)	0.133(7)
5796.94(4)	5796.904(17)	0.124(7)	7237.68(8)	7237.83(10)	0.087(5)
5802.76(10)	5802.89(5)	0.035(2)	7268.44(14)	7268.46(5)	0.038(2)
5829.89(24)	5829.49(4)	0.013(1)	7342.25(11)	*n*	0.060(3)
5860.13(3)	5860.12(3)	0.155(8)	7377.0(3)	*n*	0.021(2)
5879.03(24)	5879.42(3)	0.026(2)	7407.73(11)	*n*	0.065(5)
5882.6(6)	*n*	0.009(2)	7693.398(11)	7693.407(4)	3.3(2)
5923.42(7)	*n*	0.043(2)	7724.034(7)	7724.036(4)	26.8(1)

[a]*d* means doubtful line.
[b]*n* means not in level scheme, *m* means multiple placed in level scheme.
[c]Intensity not measured.

B. Level scheme

A level scheme of 50 levels was constructed using previously well established levels and extending it by means of the Ritz combination principle. Table II shows the level energies and for each level the spin and parity assignments, the depopulating transitions with their intensities, and the corresponding populated levels. Only the statistical error of the level energies is given in Table II. To obtain the fi-

TABLE II. Deduced level energies and spin and parity assignments. Also indicated are the populated levels and the corresponding γ transitions with their intensities.

Level energy[a] (keV)	J^{π}	Populated level (keV)	Transition energy[b] (keV)	Intensity/100n
0.0	3^{+}			
30.6383(9)	2^{+}			
972.38(4)	0^{+}	0	31	d
		31	942	1.29
1013.626(12)	3^{+}			
		0	1014	2.7
		31	983	4.4
1372.95(3)	1^{+}			
		0	1373[d]	0.15
		31	1342	0.99
		972	401	0.63
1620.32(5)	1^{+}			
		31	1590	1.63
		972	648[d]	0.07
1622.92(3)	$2^{+}(3^{+})$			
		0	1623	4.6
		31	1592	0.36
2138.916(13)	2^{+}			
		0	2139	2.22
		31	2108	2.84
		1014	1126	0.38
2201.46(4)	1^{+}			
		31	2171	0.45
2271.767(19)	4^{+}			
		0	2272	2.15
2486.177(19)	2^{+}			
		0	2486	0.177
		31	2456[d]	0.037
		1620	866	0.54
2565.68(8)	$1^{\pm},2^{\pm},3^{+}$			
		31	2535	0.084
		1620	945	0.24
2582.0(3)	5^{+}			
		0	2582	0.048
2656.09(4)	4^{+}			
		1014	1642	0.30
2987.53(13)	$3^{+}(1^{+})$			
		0	2988	0.32
		1014	1975[d,m]	0.025
		1623	1365	0.38
3296.39(3)	3^{+}			
		31	3265	0.42
		1623	1673	0.23
3347.191(13)	2^{+}			
		0	3347	0.50
		31	3317	0.025
		1373	1975[d,m]	0.025
3465.293(13)	4^{-}			
		0	3465	7.0
		1014	2451	0.388
		2272	1194	0.56

TABLE II. (*Continued.*)

Level energy[a] (keV)	J^{π}	Populated level (keV)	Transition energy[b] (keV)	Intensity/100n
3591.449(6)	3^-			
		0	3591	4.66
		31	3561	0.93
		1014	2578	2.21
		1623	1968	0.096
3670.77(3)	3^+			
		31	3640	0.073
		1623	2048	0.072
3709.21(3)	$2^+,3^+$			
		0	3709	0.450
		31	3678	0.308
3875.781(10)	2^-			
		0	3875	2.73
		972	2903[d]	0.011
		1014	2862	0.038
		1373	2503	0.161
		1620	2255	0.55
3900.993(24)	$(1,3,5)^+$			
		0	3901	0.230
		1014	2887	0.227
		1623	2277[d,m]	0.04
3935.583(18)	2^+			
		0	3935	0.325
		31	3905	0.200
		1014	2922	0.282
		1623	2313[d]	0.035
4244.41(9)	2^+			
		31	4213	0.056
		1014	3231	0.027
4461.92(8)	$1-5$			
		0	4462	0.042
		1014	3448	0.032
		2486	1975[d,m]	0.025
4596.51(4)	1^+			
		0	4596	0.124
		31	4566	0.0274
		972	3624	0.086
		1623	2974	0.024
4691.100(6)	3^-			
		0	4691	4.60
		31	4660	2.57
		1623	3068	0.081
		2139	2552	0.094
		2272	2419	0.136
4764.913(11)	2^-			
		0	4764	0.91
		31	4734	5.5
		1014	3751[m]	0.035
		1373	3392	0.57
		2139	2626	1.37
		2201	2564[d,m]	0.097
		2486	2277	0.04
		3591	1173	0.39

TABLE II. (*Continued.*)

Level energy[a] (keV)	J^{π}	Populated level (keV)	Transition energy[b] (keV)	Intensity/100n
4903.576(8)	$2^-(4^-)$			
		0	4903	3.06
		1014	3890	0.227
		2656	2247[d]	0.040
5015.42(5)	3^+			
		0	5016[d]	0.0034
		31	4984	0.113
		1014	4002	0.135
		2272	2744	0.044
		3296	1720[d,m]	0.08
5134.839(11)	3^-			
		0	5134	2.98
		31	5104	0.390
		972	4162[m]	0.019
		1014	4120[m]	0.040
5176.97(5)	$1^+,2^{\pm},3^+$			
		0	5176	0.070
		1014	4162[m]	0.019
		1373	3804	0.011
		2486	2691	0.029
5377.81(4)	$1^+,2^{\pm},3^{\pm},4^{\pm},5^+$			
		0	5377	0.080
		1623	3755	0.043
5442.276(11)	$2^-(1^-)$			
		0	5442	0.0148
		31	5411	2.04
		1373	4069	0.157
		1620	3821	0.033
		2139	3303	1.14
		2566	2876	0.116
		3465	1975[d,m]	0.025
5741.115(13)	$1^+,2^{\pm},3^{\pm},4^+$			
		31	5710	0.56
		1620	4120[d,m]	0.040
		2486	3255	0.022
		3465	2277[d,m]	0.04
5797.548(21)	2^-			
		0	5797	0.124
		31	5766	0.382
		1014	4783	0.011
		1373	4424	0.363
5860.78(3)	$1^+,2^{\pm},3^+$			
		0	5860	0.155
		31	5830	0.0126
		1623	4237[m]	0.060
		2139	3722	0.030
		2201	3659	0.064
6019.61(3)	$1^+,2^{\pm},3^{\pm},4^+$			
		0	6019	0.187
		31	5988	0.0228
		1014	5005	0.048
		1623	4396	0.058

TABLE II. (*Continued.*)

Level energy[a] (keV)	J^π	Populated level (keV)	Transition energy[b] (keV)	Intensity/100n
6198.880(11)	$2^+,3^\pm,4^+$			
		0	6198	0.67
		1014	5185	0.0297
		1623	4576	0.304
		2139	4060	0.030
		2272	3927	0.023
6316.795(10)	2^+			
		0	6316	2.02
		972	5344	0.0171
		1014	5303	0.474
		2272	4045	0.0228
		2566	3751[m]	0.035
		3296	3020	0.073
		3591	2725	0.021
		4597	1720[d,m]	0.08
6419.84(12)	$1^\pm,2^\pm,3^+$			
		0	6420	0.0057
		972	5447[c]	0.0354
		2139	4280	0.165
		2201	4218	0.027
		3465	2955[c]	0.23
6441.448(15)	$3^+,4^\pm5^+$			
		0	6441	0.66
		1014	5427	0.087
		2272	4169	0.122
		2582	3859	0.046
6623.08(6)	$1^+,2^\pm,3^\pm,4^+$			
		0	6622	0.193
		31	6592	0.164
		2988	3635	0.010
		4904	1720	0.08
6651.17(4)	$1^+,2^\pm,3^+$			
		31	6620	0.236
		1373	5278	0.0205
		2139	4512	0.084
		2566	4085	0.0080
6756.67(6)	$2^+,3^\pm$			
		31	6725	0.086
		2272	4485	0.071
		2486	4270	0.054
		2656	4102	0.016
		2988	3769	0.0126
		3347	3409	0.023
		3876	2881	0.027
6893.70(3)	$2^+,3^\pm$			
		31	6862	0.173
		1014	5879	0.0262
		2139	4754	0.381
		2272	4621	0.191
		2656	4237	0.060
		3671	3223	0.049
		3876	3017	0.058
		4765	2129	0.340

TABLE II. (Continued.)

Level energy[a] (keV)	J^π	Populated level (keV)	Transition energy[b] (keV)	Intensity/100n
7176.49(4)	$1^+,2^\pm,3^+$			
		0	7176	0.133
		1014	6162	0.0126
		1373	5803	0.0354
7269.48(7)	$2^+,3^\pm,4^+$			
		0	7268	0.0377
		31	7238	0.087
		1014	6255	0.0137
		2139	5130	0.107
		2656	4613	0.0160
		3671	3599	0.151
		4244	3024	0.052
7725.180(5)	$2^+,3^+$			
		0	7724	26.81
		31	7693	3.27
		972	6752	0.058
		1014	6711	0.90
		1373	6351	0.110
		1623	6101	2.58
		2139	5586	1.10
		2201	5523	0.064
		2272	5453	0.168
		2486	5238	0.258
		2582	5142	0.0148
		2656	5069	0.173
		2988	4737	0.448
		3296	4428	0.81
		3347	4378	0.434
		3465	4260	6.8
		3591	4133	6.9
		3671	4054	0.143
		3709	4016	0.73
		3876	3849	3.12
		3901	3824	0.56
		3936	3789	0.87
		4244	3481	0.119
		4462	3263	0.105
		4597	3129	0.236
		4691	3034	8.8
		4904	2821	3.87
		5015	2710	0.69
		5135	2590	4.22
		5177	2548	0.148
		5378	2347	0.155
		5442	2283	4.75
		5741	1984	1.07
		5798	1928	1.20
		5861	1865	0.46
		6020	1705	0.39
		6199	1526	1.80
		6317	1408	3.1
		6420	1305	0.19

TABLE II. (*Continued.*)

Level energy[a] (keV)	J^{π}	Populated level (keV)	Transition energy[b] (keV)	Intensity/100n
		6441	1284	1.14
		6623	1102	0.73
		6651	1074	0.57
		6757	969	0.42
		6894	831	1.35
		7176	549	0.23
		7269	456	0.29

[a]Only the statistical error is given; to obtain the total errors an additional systematic error of 11 ppm has to be added in quadrature.
[b]d means doubtful line, m means multiple placed in level scheme.
[c]The decay to the 972 keV 0^+ level and to the 3465 keV 4^- level is unlikely. Therefore, one of the transitions might be placed by chance.
[d]Intensity not measured.

nal error an additional systematic error of 11 ppm has to be added in quadrature. The spin and parity assignments are based on previous publications[3] and on the assumption that only $E1$, $E2$, and $M1$ transitions have been observed. The intensity balance is good for most of the levels. The difference between population and depopulation is less than $1.3/100n$ in all cases. The total intensity leaving the capture state is $(102\pm1)\%$ and agrees with the total intensity of $(101\pm1)\%$ reaching the ground and the first excited state (the intensity of the 31 keV line is not known). The intensity of the 1779 keV decay line, which is known to be 100%,[3] is determined to be $(112\pm10)\%$.

V. DISCUSSION

A. Comparison with other experimental work

The present level scheme contains one level (2566 keV) which has not yet been reported elsewhere. Four additional levels (2582, 4462, 6420, and 6651 keV) have been observed for the first time in the (n,γ) reaction. The levels at 3105, 3541, 4997, 5188, 5344, 6831, 6853, 6968, and 7342 keV given by Ishaq *et al.*[5] or by Sushkov *et al.*[20] could not be identified by the present work. Many new gamma branchings have been found, and the errors of the level energies have been considerably reduced compared to previous values.[3] The branching ratios are in good agreement with previous work. Some previous observed weak branchings have not been found because the corresponding lines are masked by other lines (e.g., $1620\rightarrow0$). Figure 3 shows the difference of the recommended calibration energies of this work (Table I, column 2) to the values given by Stelts and Chrien.[7] The errors shown are the statistical errors of both data sets with no systematic error included. The most pronounced deviations are in the energy range of 2.0–3.5 MeV where the values of Stelts and Chrien are systematically lower than our values. It should be noted, however, that all deviations are within the systematic error of 200 eV given by Stelts and Chrien. The deviations in the energy region below 3.5 MeV could be due to the energy calibration used by Stelts and Chrien, which is based on the chlorine energies given by Spits and Kopecky.[17] These values in turn depend on gamma energies of nitrogen,[18] which have been revised in the meantime.[19]

Recently a new set of ^{28}Al energies has been published by Sushkov *et al.*[20] Comparison of these values to those of the present work shows systematic deviations up to about a maximum of 100 eV for some energy regions. It should be noted, however, that the final errors given by Sushkov *et al.*[20] do not account for remaining nonlinearities. Assuming that the uncertainties of the values given in Ref. 20 owing to remaining nonlinearities are in the same order of magnitude as in the present work, reasonable agreement is achieved between the two data sets.

B. Statistical aspects of the level scheme

Figure 4 shows the number $N(E)$ of all levels with spin values J between 1 and 4 up to the energy

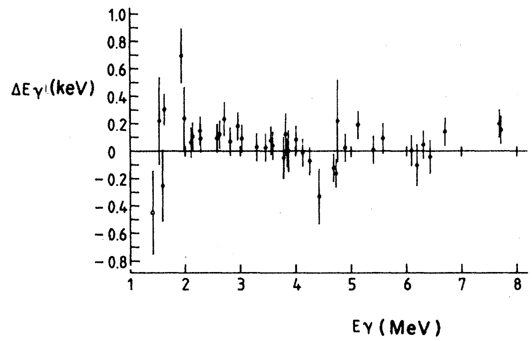

FIG. 3. Difference between the present values of the γ-ray energies and those given by Stelts and Chrien (Ref. 7).

E as a function of E. The smooth curve is the integral over the level density $\Phi(E)$, which, according to the constant temperature Fermi gas model,[21] is given by

$$\Phi(E)=\sum_{J=1}^{4}\frac{1}{T}f(J)\exp\left[\frac{E-E_0}{T}\right]$$

with

$$f(J)=\exp(-J^2/2\sigma^2)-\exp[-(J+1)^2/2\sigma^2]$$

and

$$\sigma=2.8 \text{ (Ref. 21)}.$$

Here, T is the nuclear temperature, E_0 is the pairing energy, and J is the level spin. T and E_0 are determined using the level density $\Phi_B=53\pm6$ MeV^{-1} for $1^{\pm}$, $2^{\pm}$, $3^{\pm}$, and $4^{\pm}$ levels at the neutron binding energy which was obtained from the value 45 ± 5 MeV^{-1} for 1^{+}, $2^{\pm}$, $3^{\pm}$, and 4^{+} levels given in Ref. 22 and the level density $\Phi_2=5.5\pm0.4$ MeV^{-1} at 2 MeV which was calculated by counting the levels with $1\le J\le 4$ between 1 and 3 MeV. The resulting parameters are $T=2.5\pm0.4$ MeV and $E_0=-4.8\pm0.4$ MeV. By integrating $\Phi(E)$ one finds:

$$N(E)=\sum_{J=1}^{4}f(J)\exp\left[\frac{E-E_0}{T}\right]+c\ ,$$

where c is determined by $N(0)=1$. The excellent agreement up to 4 MeV indicates the completeness of the level scheme up to this energy.

Figure 5 shows the sum of the intensities $I(E)$ of the primary transitions with energies between E and the binding energy E_B as a function of E in a similar way as presented by Tielens *et al.*[23] For comparison, theoretical estimates for the total intensity $I(E)$ are given, which are obtained by

$$I(E)=c'\int\Phi(E_B-E')g(E')dE'\ ,$$

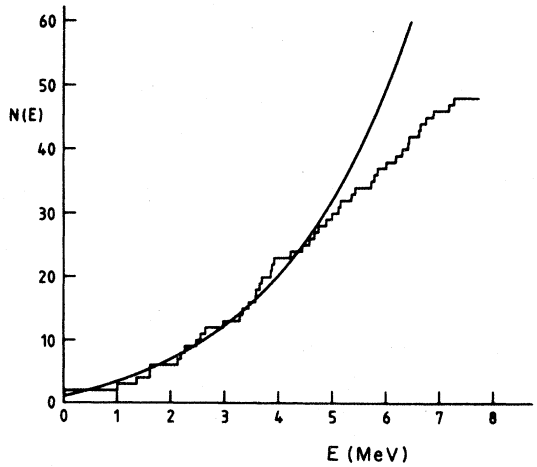

FIG. 4. Number of levels $N(E)$ up to the energy E as a function of E. The smooth curve is the theoretical expectation according to the constant temperature Fermi gas model.

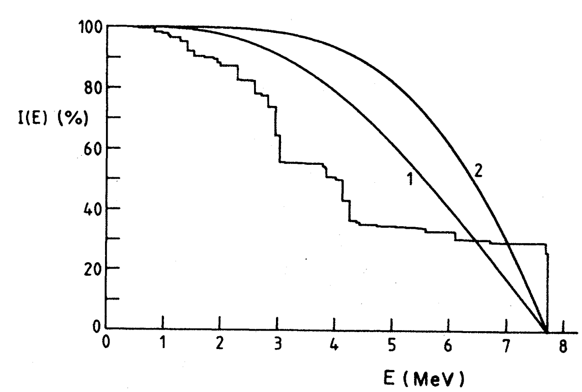

FIG. 5. Sum of the intensities of primary transitions with energies between E and the binding energy E_B as a function of E. Curves 1 and 2 are the theoretical expectations according to the single particle ($\propto E^3$) and the giant dipole resonance model ($\propto E^5$), respectively.

where $g(E)=E^3$ for curve 1 and $g(E)=E^5$ for curve 2, according to the single particle and the giant dipole resonance model,[24] respectively. The parameter c' is determined by the condition $I(0)=100\%$. The agreement is poor for both models, which is probably due to nuclear structure effects. The step in the experimental function $I(E)$ at $E=4$ MeV is due to the lowest levels with negative parity and the step at $E=3$ MeV can be attributed to the lowest single particle excitations of the core (^{26}Mg) of the nucleus ^{28}Al. Obviously, the level density is too low to cancel such structures by the statistical distribution.

ACKNOWLEDGMENTS

The financial support of the Bundesministerium für Forschung und Technologie is gratefully acknowledged. One of us (C.H.) thankfully acknowledges support by the South African Atomic Energy Board, Pelindaba. We gratefully acknowledge the fruitful comments of Professor P. M. Endt and Professor C. van der Leun.

*Present address: South African Atomic Energy Board, Pelindaba, Pretoria, South Africa.

[1]F. E. H. van Eijkern, G. A. Timmer, F. Meurders, and P. W. M. Glaudemans, Z. Phys. A 278, 337 (1976).

[2]B. J. Cole, A. Watt, and R. R. Whitehead, J. Phys. G 1, 213 (1975).

[3]P. M. Endt and C. van der Leun, Nucl. Phys. A310, 1 (1978).

[4]R. Hardell, S. O. Idetjärn, and H. Ahlgren, Nucl. Phys. A126, 392 (1969).

[5]A. F. M. Ishaq, A. H. Colenbrander, and T. J. Kennett, Can. J. Phys. 50, 2845 (1972).

[6]L. W. Nichol, A. H. Colenbrander, and T. J. Kennett, Can. J. Phys. 47, 953 (1969).

[7]M. L. Stelts and R. E. Chrien, Nucl. Instrum. Methods 155, 253 (1978); and private communication.

[8]P. P. J. Delheij, A. Girgin, K. Abrahams, H. Postma, and W. J. Huiskamp, Nucl. Phys. A341, 21 (1980).

[9]H. R. Koch, H. G. Börner, J. A. Pinston, W. F. Davidson, J. Faudou, R. Roussille, and O. W. B. Schult, Nucl. Instrum. Methods 175, 401 (1980).

[10]D. D. Warner, W. F. Davidson, and W. Gelletly, J. Phys. G 5, 1723 (1979).

[11]P. Hungerford, W. D. Hamilton, S. M. Scott, and D. D. Warner, J. Phys. G 6, 741 (1980).

[12]B. Krusche, K. P. Lieb, H. Daniel, T. v. Egidy, G. Barreau, H. G. Börner, R. Brissot, C. Hofmeyr, and R. Rascher, Nucl. Phys. (to be published).

[13]E. G. Kessler, R. D. Deslattes, A. Henins, and W. C. Sauder, Phys. Rev. Lett. 40, 171 (1978).

[14]K. Debertin, Nucl. Instrum. Methods 158, 479 (1979).

[15]Y. Tokunaga, private communication.

[16]G. F. Thomas, D. E. Blatchley, and L. M. Bollinger, Nucl. Instrum. Methods 56, 325 (1967).

[17]A. M. J. Spits and J. Kopecky, Nucl. Phys. A264, 63 (1976).

[18]J. B. Marion, Nucl. Data A4, 301 (1968).

[19]R. C. Greenwood and R. G. Helmer, Nucl. Instrum. Methods 121, 385 (1974).

[20]P. A. Sushkov, V. L. Alexeev, L. P. Kabina, and D. D. Warner, Leningrad Nuclear Physics Institute Report LNPI 644, 1981.

[21]A. Gilbert and A. G. W. Cameron, Can. J. Phys. 43, 1446 (1965).

[22]S. F. Mughabghab and D. I. Garber, Brookhaven National Laboratory Report BNL-325, 1973.

[23]T. A. A. Tielens, J. Kopecky, F. Stecher-Rasmussen, W. Ratynski, K. Abrahams, and P. M. Endt, Nucl. Phys. A376, 421 (1982).

[24]P. Axel, Phys. Rev. 126, 671 (1962).